

# Plasma Electrolytic Oxidation Coatings on Aluminum Alloys: Microstructures, Properties, and Applications

Lord Famiyeh<sup>1</sup> and Xiaohu Huang<sup>2\*</sup>

<sup>1</sup>Department of Chemical and Environmental Engineering, University of Nottingham Ningbo China, China

<sup>2</sup>Institute of Materials Research and Engineering, Agency for Science, Technology and Research (A\*STAR), Singapore

**\*Corresponding author:** Xiaohu Huang, Institute of Materials Research and Engineering, Agency for Science, Technology and Research (A\*STAR), Singapore, Email: [huangxh@imre.a-star.edu.sg](mailto:huangxh@imre.a-star.edu.sg)

**Received Date:** October 29, 2019

**Published Date:** November 06, 2019

## Abstract

Aluminum (Al) and its alloys are widely used in many industries, and anodic oxidation (AO) and plasma electrolytic oxidation (PEO) are two of the most important technical routes to improve their corrosion resistance and mechanical properties. This review paper covers both AO and PEO of Al alloys, in order to facilitate a comparison between the two technologies. A general overview of AO and PEO is provided. Then the focus is on PEO coatings, including the microstructure of PEO coatings, the effect of various PEO process parameters on the microstructure and properties of the coating. An attention is paid to the corrosion resistance and mechanical properties of PEO coatings on aluminum and its alloys. Finally, the applications of PEO coatings on Al alloys are summarized. The review intends to give a balanced coverage on recent development on PEO process and coatings, and to stimulate more research and industry interests in PEO coatings.

**Keywords:** Aluminum alloys; Plasma electrolytic oxidation; Anodic oxidation; Microstructure; Corrosion resistance; Mechanical properties

## Introduction

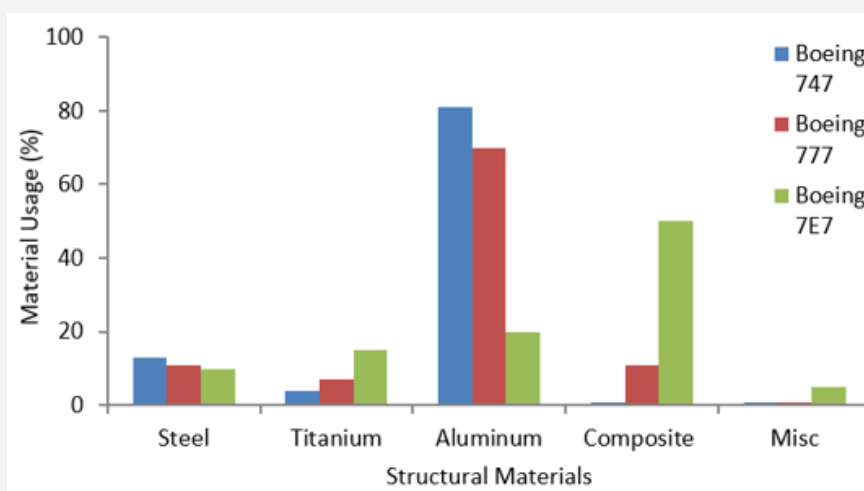


**Figure 1:** Approximate materials usage in Boeing commercial aircrafts [7].

The aerospace industry demands that the materials used for making aircrafts meet the required specifications of increased resistance to fatigue and corrosion, improved fracture toughness,

and have high strength-to-weight ratio because of their condition of service [1,2]. Aluminum and its alloys have been the primary choice of materials in the aerospace industry since the late 1920s. Today

they constitute about 70-80% of many modern aircrafts due to their high strength-to-weight ratio, easy workability, and low prices [3-6]. For example, aircrafts such as Airbus A340/A330 and Boeing 757 have their major components and load bearing structures

made of aluminum alloys [7]. Although polymer composites have emerged as competitive materials in the manufacturing of aircrafts, aluminum and its alloys remain the most widely used materials in the aircraft industry, as shown in Figure 1.

**Table 1:** Aluminum alloys and their applications in the aircraft industry [1,8-9].

Products	Strength Levels	Alloys/Temper	Applications
Plate	High strength	7150-T7751, 7150-T7751, 7150-T7751, 7150-T7751	Upper wing covers
Sheet	Damage tolerant	2024-T3, 2524-T3/351	Fuselage/pressure cabin skins, lower wing skins
Extrusions	High strength	7075-T73511, 7075-T79511, 7150-T6511, 7175-T79511, 7055-T77511, 7055-T79511	Fuselage stringers and frames, upper wing stringers, floor beams seat rails

The aluminum alloys in the series of 2xxx (Al-Cu-Mg) and 7xxx (Al-Zn-Mg-Cu), for example, 2024 and 7075 respectively are the most widely used materials in the manufacturing of aircrafts. Selected aluminum alloys/temper and their applications in the aircraft industry are listed in the Table 1.

Generally, the 7xxx aluminum alloys have the highest tensile strength (~520-620MPa) in comparison to other aluminum-based alloys, the next in the rank is 2xxx alloys (~380-520MPa) [8]. The high strength of 7xxx alloys particularly 7075 and 7150 is an important requirement because of their wide usage for load bearing structures in aircrafts. The 7xxx alloys derive their high strength from precipitation of  $\eta$ -phase ( $MgZn_2$ ) and its precursor forms [10,11]. However, the presence of coarse secondary phase particles such as  $Al_7Cu_2Fe$ ,  $Mg_2Si$ , and  $Al_2CuMg$  (S-phase) could leads to a reduction in tensile ductility and fracture toughness [11,12]. The tensile strength, ductility and fracture toughness of aluminum alloys can be enhanced by controlling the level of impurity elements such as iron and silicon or adopting heat treatment strategies and tempers [7]. Furthermore, fatigue challenges associated with some aluminum alloys, for example thick 7010 and 7050 plate are a major concern in the aerospace industry. This requires much attention from aluminum alloy producers because this problem is mostly caused by crack initiation due to the presence of micro porosity arising from DC casting process [13]. The fatigue behavior of such alloys can be enhanced through optimization of chemical composition, processing and casting parameters, and by employing coating techniques [13].

Despite the unique properties of aluminum and its alloys and their ability to form thin natural oxide protective layers, their susceptibility to different kinds of local corrosions such as stress corrosion cracking, pitting corrosion, intergranular corrosion, and exfoliation corrosion under extreme conditions is a major challenge in the aerospace industry [14,15]. Moreover, the 7xxx alloys despite their popularity in the aerospace industry because of their high strength comparable to many steels, moderate fatigue strength, and reasonable machinability, their applications are restricted because of their high susceptibility to exfoliation corrosion and stress corrosion cracking (SCC) at peak-aged condition [4,10]. The presence of secondary phase inter-metallics in the microstructure of high strength aluminum alloys in the series of 7xxx (Al-Zn-Mg-Cu) and 2xxx (Al-Cu-Mg) makes them highly susceptible to SCC attack than most of the low strength alloys, particularly those in the

series of 3xxx (Al-Mn), 4xxx (Al-Si), 5xxx (Al-Mg), and 6xxx (Al-Mg-Si) [15,16]. The corrosion mechanism of aluminum and its alloys in the aircraft industry has not been fully studied and therefore much attention and dedicated work is required.

Conventionally, aluminum alloys used in aircraft industry requires SCC protection in order to ensure the safety of the aircraft and its passengers. This can be accomplished by restricting the alloy strength levels, using stress relief treatments, or employing surface treatment techniques such as anodic oxidation (OA), plasma electrolytic oxidation (PEO), and ion vapor deposition [8,15]. The surface treatment methods are the most effective way to enhance the corrosion resistance and hardness of aluminum and aluminum alloys. And surface treatment based on electrochemical methods is simple and rapid and exhibits high repeatability. For example, aluminum alloy, 2024-T3 anodized in sulphuric acid was found to exhibit a significant improvement in corrosion resistance compared to the bare 2024-T3 [15]. The oxide ( $Al_2O_3$ ) layer formed on aluminum and its alloys provide surface protection against corrosion due to its capacitive behavior. Among the electrochemical surface treatment methods, PEO has attracted considerable interest in recent years because of its numerous advantages over other methods such as physical vapor deposition (PVD), chemical vapor deposition (CVD), ion beam assisted deposition, and sol-gel technique [18]. The PEO technique is effective on aluminum and aluminum alloys and it generates thick ceramic coatings with outstanding characteristic of adhesion to substrate, uniformity and compactness which improves the corrosion resistance, fatigue strength, wear resistance, and surface hardness [14,17,19]. Furthermore, PEO process is environmental friendly, easy to control, less expensive, and a single-step technique that can be employed for surface treatment of materials with complex 3D surface geometry and wide range of sizes, which is not possible in the case of many other surface treatment methods [20,21].

## Discussion

Anodic oxidation and plasma electrolytic oxidation are electrochemical surface treatment methods that have been widely employed for surface modification of aluminum and its alloys in order to make them suitable for certain applications. In this paper much attention is paid on PEO treatment of aluminum and its alloys because of its numerous advantages over other surface treatment techniques and increasingly interest in both academic research and industry.

## Anodic oxidation

Anodic oxidation was developed in the early 1930s. It has been widely applied for surface treatment of light metals (Al, Mg, and Ti) and their alloys in order to increase their usage specifically in areas that require some level of corrosion protection and wear resistance [22,23]. In anodic oxidation, the setup of the electrochemical cell consists of anode and cathode which are working electrode (sample to be anodized) and auxiliary electrode (e.g. platinum mesh wire), respectively. The electrodes are connected to DC power source as shown in Figure 2. The reactions that occur at the anode and the cathode are shown in equations (1-5). Typically, the AO technique normally operates at a constant cell voltage which ranges from 20 to 80 V and at a low current density (1-10 Adm<sup>-2</sup>) [24]. The schematic equipment of anodic oxidation is also shown in Figure 4.

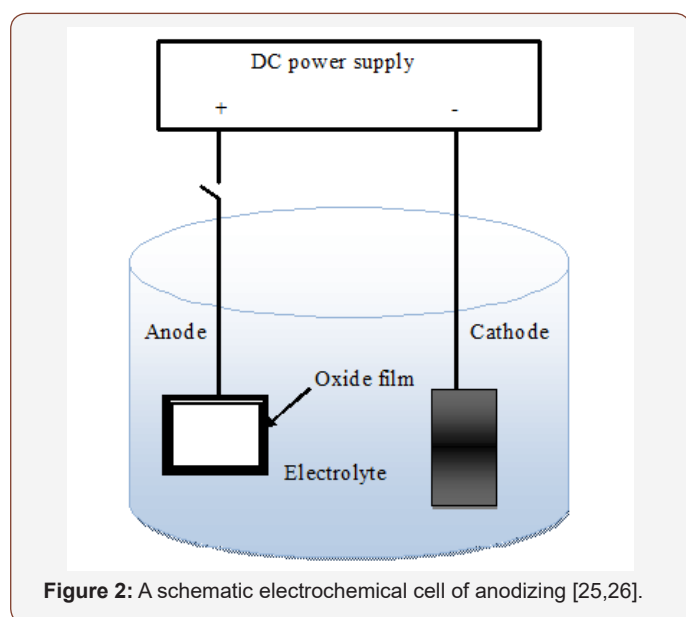


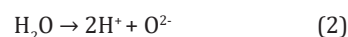
Figure 2: A schematic electrochemical cell of anodizing [25,26].

In anodic oxidation the electrolyte used is acidic, this can be either sulphuric acid, chromic acid, phosphoric acid, oxalic acid, or boric acid used singly or in combination [27-31]. Prior to anodizing, samples are pretreated by polishing their surfaces with SiC paper and degreased with alcohol or acetone and cleaned with deionized water [32].

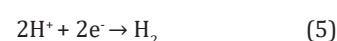
The mechanism of anodic oxidation of metals and alloys, for example, aluminum and its alloys involve simultaneous formation and dissolution of the alumina (Al<sub>2</sub>O<sub>3</sub>) as shown in equation (3) and (4), respectively [33]. The dissolution process generates pores which are filled with electrolyte resulting in the formation of new aluminum oxides that subsequently grow to form amorphous alumina layers consisting of a thin barrier region and a thicker porous region with linear pores on the oxide surfaces [33]. The dissolution-based mechanism for pore formation and growth has been disputed by many experiments, this include oxygen isotope (<sup>18</sup>O) studies. In pore formation and oxide growth via anodic oxidation the mechanism has been proposed to be governed by electric-field interface evolution, mechanical stress-guided repulsion and viscous flows of the oxide species [34]. The electric-field assisted mechanism involves oxide decomposition

which results in direct ejection of molten aluminum (Al<sup>3+</sup>) into the solution followed by oxide formation via transport of oxygen ion (O<sup>2-</sup>) at oxide/electrolyte interface and Al<sup>3+</sup> transport at metal/oxide interface in the opposite direction [35,36]. Direct ejection of Al<sup>3+</sup> from metal/oxide interface into electrolyte has been indicated by coating-ratio measurement and tracer experiments [36]. The reaction at the anode and cathode are listed below [35,36].

Anodic:



Cathodic:



The characteristics of the anodized coatings can be influenced largely by the process conditions, which include cell potential, current density, oxidation time, type of electrolyte and pH, and temperature of the electrolyte [37-39]. For example, lowering bath temperature (<25°C) produces dense and thick coatings, and increasing current density increases the film thickness, the true relationship can be very complex because excessive increase in current density increases the temperature in the film grown zone due to joule heating, this leads to oxide dissolution [40]. Furthermore, a very long anodization time decreases the film thickness and current efficiency because the rate of oxide dissolution exceeds the rate of oxide formation [40].

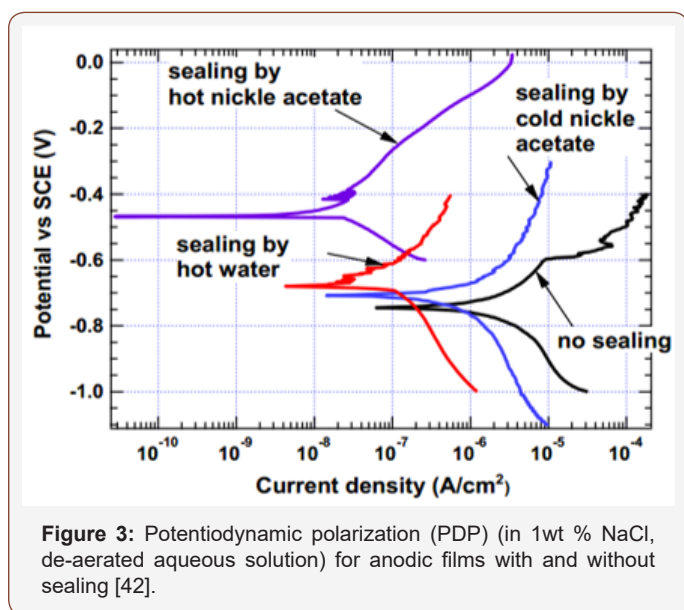
Generally, the oxide coatings formed via AO process is porous in nature with only a few micrometers in thickness and has limited elasticity and high hygroscopicity which exhibits some improvement in the corrosion and wear resistance [41-46]. For aerospace applications that requires high level of corrosion protection, sealing is required after anodizing in order to reduce surface cracking and block penetration of corrosive species [33,42]. Sealing the anodized sample can be done by immersing in hot deionized water (~95°C) for about 15 to 30 min or in hot nickel sulphate solution (5-10g/L, ~90°C) for about 20 to 30 min, hot nickel acetate (5g/L, 90°C) for 30 min, and cold nickel acetate (5 g/L, 25°C) for 30 min [33,42-45]. The effect of hot water, hot nickel acetate and cold nickel acetate sealing on corrosion performance of anodized aluminum coupons and foils was investigated by Hu et al. [42], it was found that hot nickel acetate showed the best corrosion performance as shown in Figure 3. During sealing in hot deionized water, the alumina (Al<sub>2</sub>O<sub>3</sub>) becomes hydrated to form aluminum mono-hydroxide or boehmite (equation 6) which fills the pores and seals the surface in order to prevent environmental attack and reduces corrosion [33,43,45]. According to studies conducted by El-Hameed et.al, a reduction in oxide film thickness (weight loss) was observed during the sealing process [45] (Table 2).



**Table 2:** Examples of recent studies on anodic oxidation of aluminum and its alloys.

Substrate	Operational Parameters				Electrolyte	Film Thickness [ $\mu\text{m}$ ]	Ref
	$i$ [ $\text{A}/\text{dm}^2$ ]	$v$ [V]	$t$ [min]	$T$ [ $^{\circ}\text{C}$ ]			
Al	12-Feb	100	10	40	$\text{H}_2\text{Cr}_2\text{O}_7$ (0.4M)/ $\text{SO}_4^{2-}$	1.7-2.1	31
Al	NA	22	20-May	20	$\text{H}_2\text{SO}_4$ (0.1M)/ $\text{H}_2\text{ZrF}_6$ (0-1.0wt %)	0.94-16.9	48
Al	NA	20-60	30-120	35-50	$\text{C}_2\text{H}_2\text{O}_4$ (0.3M)	NA	50
Al	NA	40	720	4	$\text{C}_2\text{H}_2\text{O}_4$ (0.3M)	50	101
AA1050	NA	17	15	NA	$\text{H}_2\text{SO}_4$ (1.0M)/ $\text{Al}_2(\text{SO}_4)_3$ (1.0g/L)	NA	32
AA1100	0.015	15	120	NA	$\text{H}_2\text{SO}_4$ (20wt %)	NA	42
AA2024	NA	10	60-200	25	$\text{H}_2\text{SO}_4$ (184g/L)/ $\text{Al}_2(\text{SO}_4)_3$ (20g/L)	NA	33
AA2024	2-Jan	15	30-60	21-35	$\text{H}_2\text{SO}_4$ (15wt %)	2.2-5.3	45
AA2024	NA	18-Oct	NA	40-60	$\text{H}_2\text{SO}_4/\text{C}_6\text{H}_8\text{O}_7$	2.7-26.3	46
AA2024	12-Feb	B-S	40	40	$\text{H}_2\text{Cr}_2\text{O}_7$ (0.4M)/ $\text{SO}_4^{2-}$	2.4-3.5	31
AA6061	2-Jan	15	30-60	21-35	$\text{H}_2\text{SO}_4$ (15wt %)	5.3-13.4	45
AA7050	2.5	0-25	40	0-5	$\text{H}_2\text{SO}_4$ (15wt %)	$23 \pm 3$	13
AA7075	15	NA	15	15	$\text{H}_2\text{SO}_4$ (15wt %)	20-Oct	43
AA7075	NA	19-26	15-30	20-50	$\text{H}_2\text{SO}_4$ (10-50g/L)/ $\text{H}_3\text{PO}_4$ (40-80)	1.2-5.0	49
AA7075	2-Jan	15	30-60	21-35	$\text{H}_2\text{SO}_4$ (15wt %)	1.8-3.3	45
AA7075	NA	14	40-90	20	$\text{H}_2\text{SO}_4$ (0.40M)/ $\text{C}_4\text{H}_6\text{O}_6$ (0.53M)/ $\text{Na}_2\text{MoO}_4$ (0.25M)	6.1-14.9	47

$i$  = current density,  $v$  = cell voltage,  $t$  = duration of anodizing,  $T$  = temperature of electrolyte, NA = not known



To prevent reduction of the film thickness and reduce hygroscopicity, the porous oxide layer could be impregnated with organic or inorganic dyes before sealing, and this could also serve as a way of coloring the anodized piece [30,41,45]. There are several researches works on anodic oxidation of aluminum and aluminum alloys, some examples of recent research work are shown in Table 2.

### Plasma electrolytic oxidation

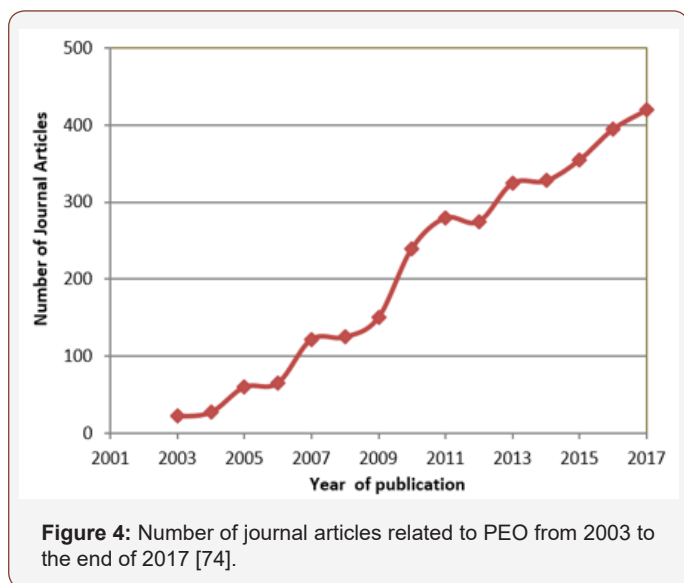
**General overview of PEO treatment:** Plasma electrolytic oxidation (PEO), also called micro-arc oxidation (MAO), anode sparks deposition (ASD), micro-plasma oxidation (MPO), and micro-arc discharge oxidation (MADO), was developed more

than four decades ago to overcome the setbacks of convectonal anodizing technique [24,29,51-100]. The purpose of PEO treatment is to achieve excellent improvement in corrosion resistance and mechanical properties of valve metals such as magnesium, aluminum, titanium, zirconium and their alloys. PEO treatment of aluminum and its alloys is the main focus of this paper. This surface engineering technique works best at a high voltage (400-700 V), which is greater than the dielectric breakdown voltage by few hundred volts [53,54]. The PEO process starts with anodizing to produce a barrier layer and then proceed to a stage where dielectric breakdown begins accompanied by ionization of the oxide material and gas evolution [54]. The electrolyte used is non-toxic alkaline (pH=7-12) free of heavy metals (Cr, Ni, V, etc.), the electrodes are immersed in the electrolyte and connected to a power source which can be in either DC, AC, unipolar pulsed or bipolar pulsed mode [30,55,56]. The choice of PEO operating conditions significantly influences the coating morphology, structure and composition and thereby affecting coatings corrosion and wear resistance properties as well as mechanical and tribological properties (Figure 4).

There has been a tremendous interest and increase in PEO coatings research in many research laboratories worldwide from 2003 to 2017, averagely there has been a continuous increase in the number of published papers, this is shown in Figure 4. Most PEO research are dedicated to optimization of process parameters to produce defect-free coatings with excellent corrosion and wear resistance, and mechanical and tribological properties of Al, Mg, and Ti and their alloys. Other research works have been dedicated to providing comprehensive understanding of the mechanism of PEO process and the impact of micro discharges on coatings

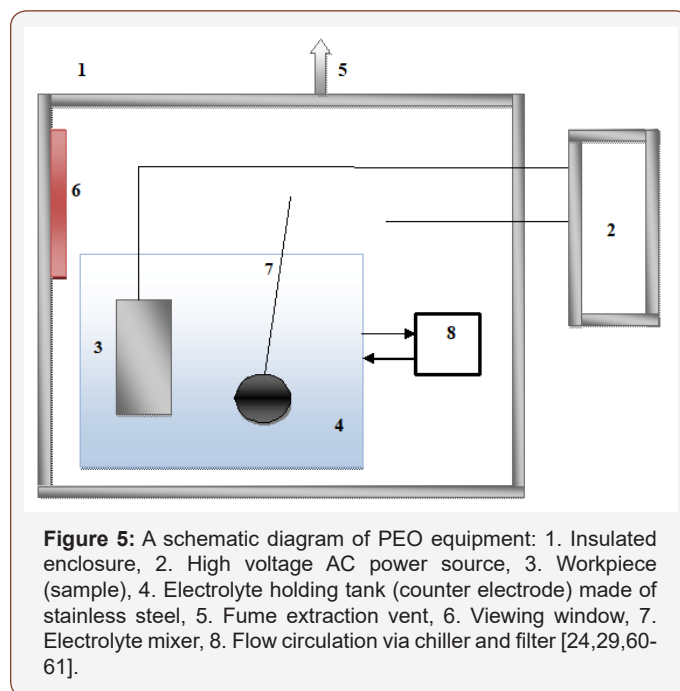


morphology, structure and phase composition. Also, the influence of additives on coating properties has been extensively investigated by many researchers.



**Experimental setup and mechanism of PEO process:** A schematic representation of typical equipment for PEO surface treatment is shown in Figure 5. The setup consists of an insulated enclosure (1) which has a viewing window (6) and fume vent (5) and it is mounted on a high voltage AC power source (2). The workpiece (3) is immersed in a stainless-steel electrolyte holding tank (counter electrode) (4) with an electrolyte mixer (7) which ensure complete mixing of the electrolyte during the PEO process. The counter electrode is connected to chiller and filter (8) to cool the system and recycle the electrolyte. The workpiece (3) and the counter electrode (4) are connected to a high voltage AC power source (2). Prior to PEO samples treatment, samples are subject to grounding and polishing with abrasive paper and degrease ultrasonically in acetone, clean with distilled water and allow drying in cold air. Also, prior to surface characterization, corrosion and mechanical properties measurement, PEO coated sample must be cleaned with distilled water and allowed to dry in air to reduce the level of electrolyte impurities on substrate surface (Figure 5).

The mechanism of the PEO process can be divided into three stages, all the three stages occur simultaneously. The first stage involves oxide formation at metal-oxide interface and migration of the electrolyte through the oxide layers towards the substrate. The second stage involves chemical dissolution of the oxide at oxide-electrolyte interface, and the third stage involve dielectric breakdown of the oxide layer at a high voltage. The dielectric breakdown produces millions of short-lived micro-discharges uniformly spread on the surface of the working electrode (sample) creating a discharge channel for direct ejection of molten aluminum ( $Al^{3+}$ ) which is oxidized, hydrolyzed, precipitated and melted on the workpiece [57,58]. At the discharge site chemical, electrochemical, thermo-dynamical, and plasma-chemical reactions occurs to modify the structure, composition and morphology of PEO oxide coatings [59].



The dielectric breakdown of the oxide layer results in a sharp increase in electric current and increase in local temperature (103K to 104K) to produce water and gas vapor which build-up pressure (~102 MPa), this leads to water oxidation and  $O_2$  evolution as shown in equation (8) [55,62]. At high temperatures transformation of  $\gamma$  to  $\alpha$ - $Al_2O_3$  phase occurs, this increases coatings hardness and wear resistance [54,60-64]. The low current efficiency (10-30%) and high energy consumption (3-26.7KWh  $\mu m^{-1}m^{-2}$ ) in PEO process is due to dielectric breakdown of the oxide layer and free radical reactions which promote electronic conductivity and oxygen evolution as shown in equations (7-8) [65,66]. The energy consumption of PEO is higher compared to hard anodizing technique. To minimize the energy consumption and enhance the efficiency of the process the oxidation time should be short and growth rate should be high (1-2 $\mu m/min$ ) [55,66].

**Microstructures of PEO coatings:** The X-ray Diffraction analysis gives a macroscopic picture on the phase of the PEO coatings. A typical example is shown in Figure 6, which reveals that PEO coatings on aluminum and aluminum alloy substrates mostly consist of a complex mixture of amorphous ( $\gamma$ - $Al_2O_3$ ) and crystalline ( $\alpha$ - $Al_2O_3$ ) alumina phases and other species incorporated into the coatings from the substrate and electrolyte. It is also possible to have other phases such as  $\eta$ - and  $\delta$ - $Al_2O_3$ , and mullite ( $3Al_2O_3 \cdot 2SiO_2$ ) in PEO coatings. Mullite is commonly present in coatings treated in a high concentrated silicate electrolyte, such coatings are good candidate for thermal barrier applications [52,64,72]. Generally, the presence of any phases,  $\alpha$ -,  $\gamma$ -,  $\eta$ -,  $\delta$ - $Al_2O_3$ , and mullite in PEO coatings increases coatings hardness compared to pure substrate and conventional AO coating [73].

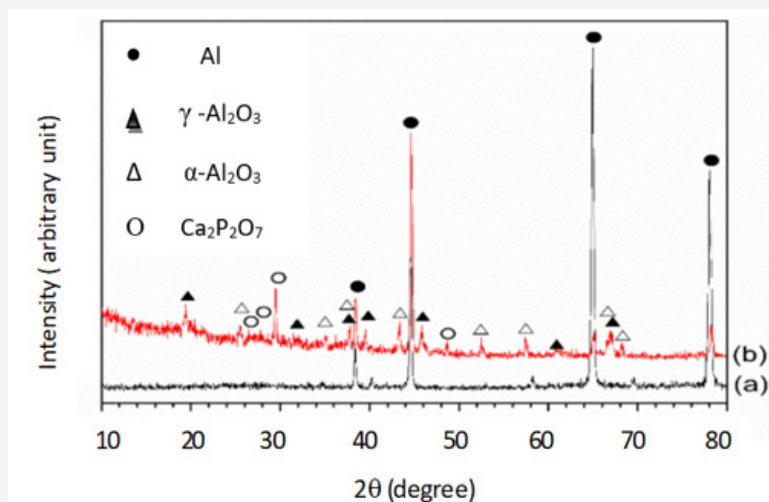


**Figure 6:** A typical X-ray spectra of PEO coating in  $(\text{Ca}(\text{H}_2\text{PO}_4)_2\text{H}_2\text{O})$  electrolyte, (a) bare AA6061, (b) PEO coated AA6061 [71].

Electron microscope characterizations reveal that a typical PEO coating on aluminum substrate consists of three layers: a porous top layer, a dense intermediate layer with low porosity, and an inner transition layer, as shown in Figure 7a [70]. Such a three-layer structure can be further visualized and analyzed by cross-sectional scanning transmission electron microscopy (STEM). As shown in Figure 7b, and the outer/external layer is consisted of both

sintered  $\text{Al}_2\text{O}_3$  and  $\text{SiO}_2$  with high porosity and large thickness, and the intermediate amorphous layer is about  $1\ \mu\text{m}$  in thickness, and the dense inner layer contains well crystallized  $\alpha\text{-Al}_2\text{O}_3$  with low porosity and is about  $1.5\ \mu\text{m}$  in thickness [52]. Generally, the dense inner layer acts as a good barrier layer for corrosion resistance and determines the thermo-mechanical and tribological properties of PEO coatings [24,29,57,66,68-69] (Figure 7).

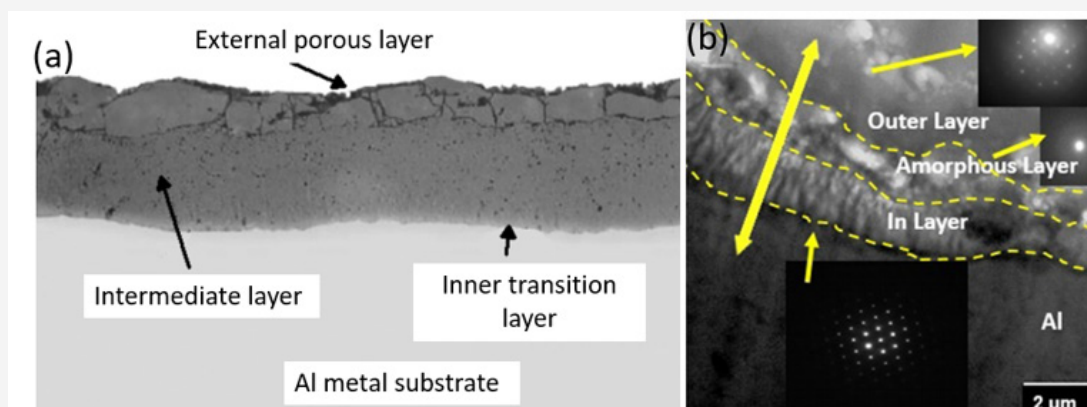


**Figure 7:** (a) A typical cross-section SEM image of PEO coatings on Al substrate [70]. (b) A typical cross-section TEM image of PEO coated AA 6061 alloy [52].

**Effect of PEO process parameters:** The microstructure and properties of PEO coatings are largely influenced by the substrate material and its composition, electrolyte and its composition, temperature of the electrolyte during the process, oxidation time, and electrical parameters [57,60,70,78-81]. Understanding how these process parameters influence PEO coatings properties is a key step towards a successful research and industrial development in this field. The effect of these parameters on coatings morphology, structure, phase composition, and corrosion and mechanical properties are summarized here.

**a) Effect of substrate materials:** The substrate material in PEO process determines the type of oxides that can be formed, which influences the properties of the coatings. For example, in the case of light metals such as Al, Mg, Ti and their alloys, the main component in the PEO coatings will be  $\text{Al}_2\text{O}_3$ , MgO and  $\text{TiO}_2$

respectively, and accordingly, the hardness of the PEO coatings ranges from 300 to 2500HV, 200 to 1000HV, and 300 to 1100HV, respectively [29,61,67,82]. Besides, the PEO coating morphology and structure also varies with the substrate composition, for example, PEO coatings prepared on aluminum alloys with high content of Si and Cu usually contain large numbers of local flaws and defects [61]. The presence of alloying elements such as Mg, Cu and Zn impedes the phase transition of  $\gamma$ -to  $\alpha\text{-Al}_2\text{O}_3$ , this leads to low coating hardness [83-84] (Figure 8).

In a recent study conducted by Sieber et al. [84], PEO coatings were prepared on different commercial high-strength aluminum alloys such as AlCu4Mg1 (EN AW-2024), AlMgSi1 (EN AW-6082), and AlZn5.5MgCu (EN AW-7075). The PEO coatings morphology and composition, hardness, and corrosion and wear resistance of the alloys were compared to coatings prepared on pure aluminum

(Al 99.5). The distribution of  $\alpha$ - and  $\gamma$ - $\text{Al}_2\text{O}_3$  phases in coatings on the different aluminum substrates were compared using EBSD-mapping, this is shown in Figure 8. It is clear that the distribution of  $\alpha$ - and  $\gamma$ - $\text{Al}_2\text{O}_3$  phases within the layers of AlZn5.5MgCu coatings is completely different from the other substrates. In AlZn5.5MgCu,  $\alpha$ - $\text{Al}_2\text{O}_3$  phase is uniformly distributed within the oxide layers and enriched at substrate/layer interface. The XRD analysis also reveals that  $\alpha$ - $\text{Al}_2\text{O}_3$  phase is less pronounced in AlZn5.5MgCu coatings, which is due to the presence of Zinc which impedes phase transformation from  $\gamma$ - $\text{Al}_2\text{O}_3$  to  $\alpha$ - $\text{Al}_2\text{O}_3$ . The distribution of  $\alpha$ - and  $\gamma$ - $\text{Al}_2\text{O}_3$  phases in coatings prepared on Al99.5, AlCu4Mg1, and AlMgSi1 coatings shows some similarity. The EDX analysis reveals that coatings prepared on the Al alloys showed some traces of alloying elements incorporated into the coatings, which influences the oxide formation and phase transformation. All coatings show some improvement in corrosion and wear resistance. However, coatings prepared on Al99.5 is found to be sensitive to chemical dissolution and this results in defective microstructure with high porosity, which contributed to its poor corrosion resistance compared to the other substrates [84].

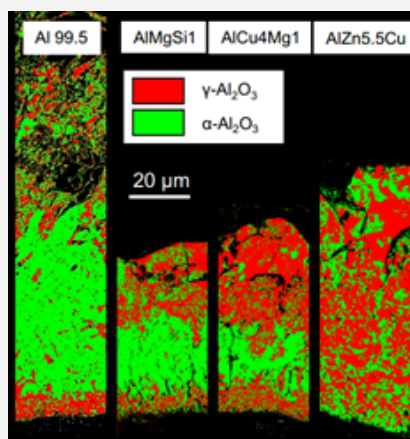


**Figure 8:** EBSD-mapping showing the distribution of  $\alpha$ - and  $\gamma$ - $\text{Al}_2\text{O}_3$  phases in PEO coatings (symmetric bipolar rectangular current pattern at 30A/dm<sup>2</sup>) on Al99.5 (in electrolyte 2 after 2 h treatment) and three high strength aluminum alloys in silicate based electrolyte (in electrolyte 2 after 2 h treatment) [84].

**b) Effect of electrolyte:** In PEO process, coatings growth rate, morphology, structure, phase composition and elemental composition are influenced by the choice of electrolyte [29,85].

Unlike conventional anodizing technique which employs acidic electrolytes, the PEO process employs environmentally friendly alkaline electrolytes, they are classified as sodium hydroxide based, silicate based, phosphate based, and aluminate based [29,52,61-62]. The composition of electrolyte affects coating properties greatly, coatings prepared on aluminum substrates in electrolyte with different compositions could show significant differences in color and properties [74]. In silicate, phosphate and aluminate-based electrolyte,  $\text{SiO}_3^{2-}$ ,  $\text{AlO}_2^-$ , and  $\text{PO}_4^{3-}$  respectively are usually incorporated into the coatings through electrophoresis under strong electric field, which affects the mechanical and tribological properties of the coatings [86].

**c) Effect of additives:** The addition of additives to the electrolyte in the PEO process greatly influences coating properties. The effects of additives such as KF,  $\text{NaAlO}_2$ ,  $\text{NH}_4\text{VO}_3$ ,  $\text{ZrO}_2$ ,  $\text{Na}_2\text{WO}_4 \cdot 2\text{H}_2\text{O}$ ,  $(\text{NH}_4)_6\text{Mo}_7\text{O}_{24} \cdot 4\text{H}_2\text{O}$ ,  $\text{K}_2\text{TiF}_6$  and  $\text{Na}_3\text{AlF}_6$  on coatings morphology, phase composition, structure, thickness, hardness, and corrosion and wear resistance have been investigated by many researchers [16,61,66,87-90]. Hwang et al. studied the effect of adding 0.08M  $\text{Na}_2\text{WO}_4$  additive into the electrolyte (KOH (0.14M)/ $\text{K}_2\text{HPO}_4$  (0.05M)) [89] and found that  $\text{WO}_3$  was incorporated into PEO coatings prepared on aluminum alloy substrate. This significantly improved the adhesion strength between substrate and coating layers. Interestingly, black ceramic coatings with large size micro pores were formed as treatment time increases. Liu et al. also showed that addition of  $\text{Na}_2\text{WO}_4$  additive to electrolyte reduces the breakdown voltage and energy consumption and increases coating density and thickness, and eventually improves the corrosion resistance [61]. The effect of  $\text{Na}_3\text{AlF}_6$  on structure and mechanical properties of PEO coatings on 6061 aluminum alloy was investigated by Wang et al. [90]. The PEO process was conducted in electrolyte of 10g/L  $\text{Na}_2\text{SiO}_3 \cdot 5\text{H}_2\text{O}$  and 1.0 g/L KOH with additive of 0.5 g/L- $\text{Na}_3\text{AlF}_6$ , and a current density of 10 A/dm<sup>2</sup> was used. Addition of  $\text{Na}_3\text{AlF}_6$  resulted in thicker ceramic coating, as shown in Figure 9. Besides, increased content of  $\gamma$ - $\text{Al}_2\text{O}_3$  and  $\alpha$ - $\text{Al}_2\text{O}_3$  were found with adding the additive. These factors lead to improvement in the micro-hardness and Young's modulus of the coatings. The hydrolysis of  $\text{AlF}_6^{3-}$  during the PEO process produced  $\text{F}^-$  which was found incorporated into PEO coatings and significantly influenced the phase composition and improved the hardness and corrosion performance [91].

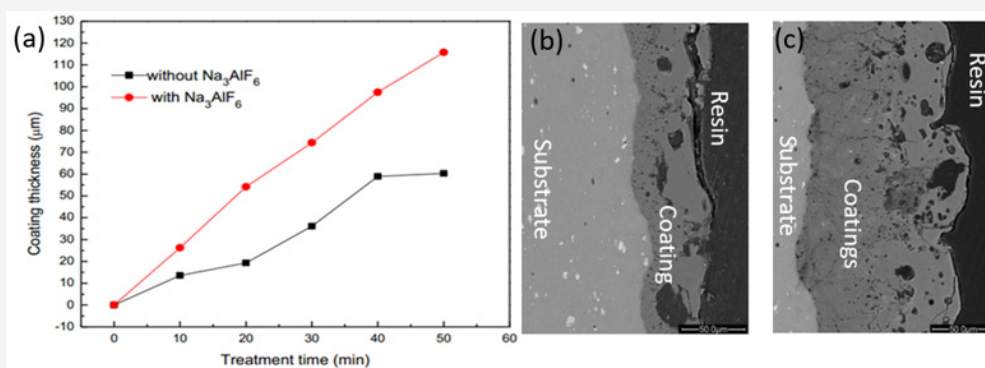


**Figure 9:** (a) PEO coatings thickness as function of time with and without  $\text{Na}_3\text{AlF}_6$ . Cross-section images of the PEO coatings (b) without  $\text{Na}_3\text{AlF}_6$  and (c) with  $\text{Na}_3\text{AlF}_6$  [90].



**d) Effect of growth time:** The oxidation of substrate and properties of the prepared PEO coatings could be influenced by growth time. As growth time increases, the coating thickness also increases while the growth rate declines. The morphology, composition, surface roughness, adhesion to substrate, and wears and corrosion resistances of PEO coatings are time dependent and therefore must be optimized during the PEO process. Sharma et al. [52] studied the effect of growth time on coatings phase composition and morphology. The temperature of the electrolyte

was controlled in the range of 33 to 38 °C and treatment time was varied from 5 to 60 min. The morphology of the coatings obtained is shown in Figure 10. In the initial stages (5-10 min) of the PEO process, it was found the coatings containing many micropores with a diameter of about 18µm. With growth time increases to 30 min and longer, the number of pores is decreased and craters with a diameter of about 90µm were formed. Similar observation was reported by Ayday et al. [92].

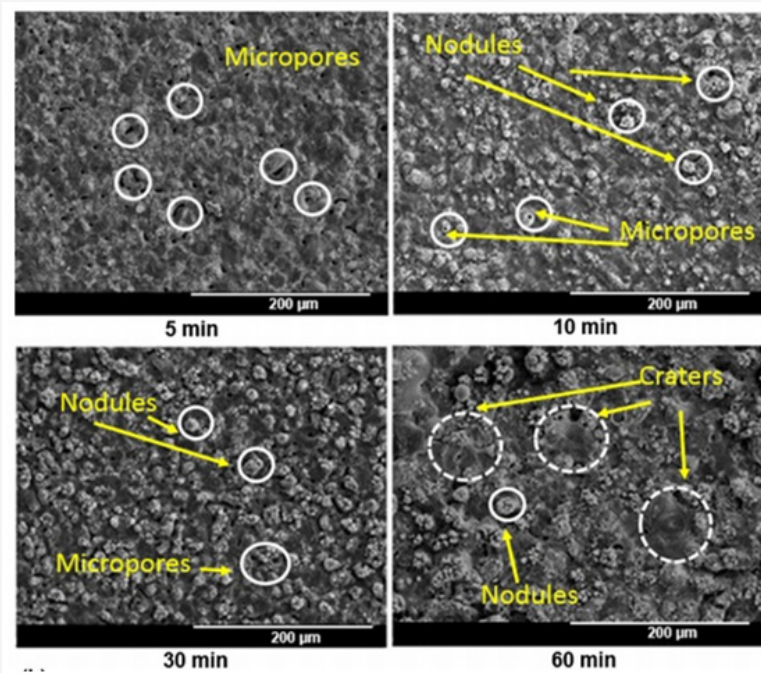


**Figure 10:** Surface Morphology of PEO coated AA 6061 alloy at different oxidation times of 5, 10, 30, and 60 min [52].

It is noteworthy to point out that  $\gamma\text{-Al}_2\text{O}_3$  was the only phase present in the coating formed in the initial stages (5-10min) of the PEO process, while  $\alpha\text{-Al}_2\text{O}_3$  appeared and remained predominant as time increases (30-60 min). This is due to the rise in temperature as a result of evolution of micro discharges during a PEO process. Generally, as PEO process time increases, the density of micro discharges decreases, and the intensity and size of micro discharges

increase. A typical photograph of the stages of micro discharges during PEO process is shown in Figure 11. The micro discharges play a significant role in the formation of PEO coatings [64], they influence crystallization and phase transformation of the coatings by localized sintering. As a result, the properties of the coatings are modified. In some instances, strong and high intensity micro discharges may cause irreversible damages to the oxide layer.

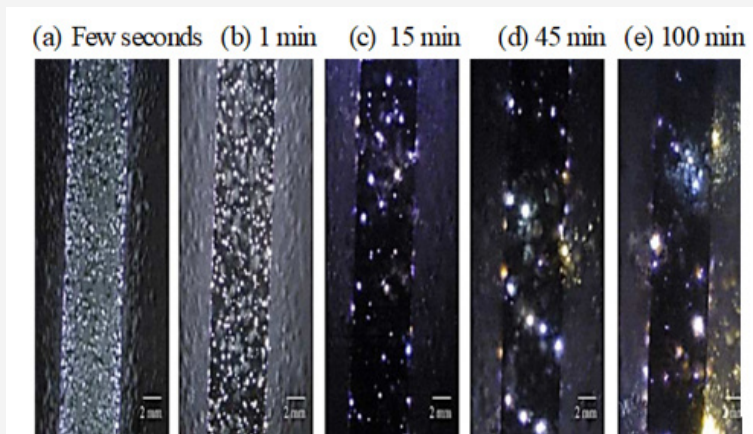
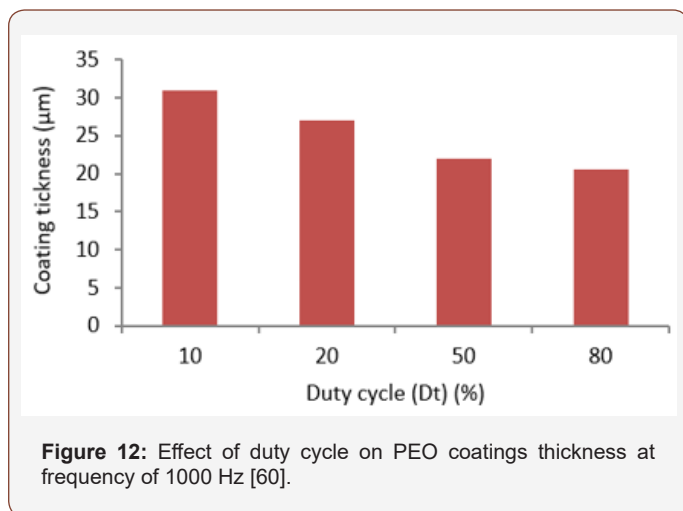


**Figure 11:** High speed video images of PEO coating showing how micro-discharges evolves with different PEO growth time [66].



**e) Effect of electric parameters:** The source of power mode used in PEO process influences coatings morphology, structure, phase composition, growth rate, hardness, and extent of porosity [61]. In DC power mode thinner coatings with no dense intermediate layer and  $\alpha$ -Al<sub>2</sub>O<sub>3</sub> phase are normally produced. Furthermore, PEO treatment operating in DC mode produces coatings at lower oxide growth rate and has greater porosity because it offers limited control and adjusting discharge characteristics is difficult compared to AC, unipolar pulsed, and bipolar pulsed mode. However, pulsed DC mode enables the discharge duration to be controlled and offers the possibility of reducing the energy usage [61,93-94]. The use of AC mode prevents electrode polarization and enables the process to be easily controlled by arc interruption. The bipolar pulsed mode has attracted attention of many researchers because it significantly improves coating properties compared to coatings produced using DC, AC, and unipolar pulsed modes. In bipolar pulsed current mode dense coatings with excellent corrosion resistance and greater coating thickness can be prepared because it reduces the number of strong plasma discharges and high temperature spikes during PEO process [61,95].

Furthermore, PEO coatings composition, microstructure, morphology and mechanical and tribological properties can be greatly influenced by duty cycle, current density, current frequency, and anodic and cathodic voltage [53,61]. Akbar et al. [60] investigated the influence of duty cycle on PEO coatings thickness. They observed a decrease in coatings thickness with duty cycle increases, as shown in Figure 12.

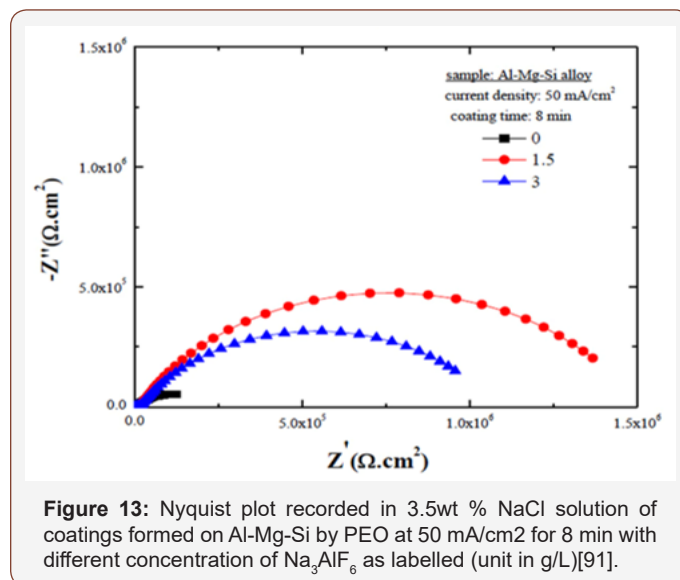


**Effect of temperature:** The temperature of the electrolyte used in PEO process can also affect the properties of coatings. At very low temperatures the oxidation potential of the substrate is poor, which reduces the PEO coating thickness and hardness. While at high temperatures dissolution of the oxide occurs, this leads to a drastic reduction in coating thickness and hardness [29]. Although in PEO process the impact of electrolyte temperature on coating properties is less compared to the convectional anodization process, it is still very necessary that temperature of the electrolyte is controlled, in most recent studies temperatures are controlled in the range of 20-40 °C [29,55,71].

## Properties of PEO coatings

**a) Corrosion Resistance of PEO coatings:** Among the light metals, Al is the second most sensitive to corrosion followed by Ti with Mg being the first. It has been demonstrated in previous studies that PEO coatings significantly improve corrosion resistance of Al and its alloys compared to those uncoated. To evaluate the corrosion performance of PEO coatings, electrochemical methods such as electrochemical impedance spectroscopy (EIS) and potentiodynamic polarization (PDP) are most widely used [16,71,81,84], and an aqueous 3.5wt% NaCl solution (similar to that of natural seawater) is used as the electrolyte. For PEO coatings intended for biocompatibility applications the corrosion performance is normally performed in Hanks solution.

The mechanism of corrosion protection of coatings can be attributed to the non-conductive nature of the oxide layer and its high dielectric constant. The alumina coatings prepared on substrates limit the flow of current and reduce the corrosion potential of the substrate. In the initial stages of immersion (in only a few minutes) the penetration of the corrosive medium is hindered by the oxide layer formed, and between 10-24 hours of immersion the corrosive medium penetrates through the pores and cracks in the coatings and remains at the substrate/coating interface leading to corrosion of the substrate, and after 24 hours the corrosion process is controlled by diffusion of the corrosion products [66]. It is important to know that improvement in corrosion resistance of PEO coatings depends greatly on the process parameters. The coatings composition, thickness, porosity and defect level also affect the corrosion behavior of PEO coating. And it is a general practice to use sealants to block the pores and micro-cracks, in order to increase the corrosion resistance [61,74] (Figure 13).



One important effective way to improve the corrosion resistance of PEO coating is by adding additives into the PEO growth electrolyte. Kaseem et al. [91] studied the influence of Na<sub>3</sub>AlF<sub>6</sub> (0, 1.5, 3 g/L) on corrosion performance of PEO coatings. Coatings were prepared on Al-Mg-Si alloy in electrolyte consisting

of  $\text{Na}_3\text{PO}_4$  (6g/L)/KOH (3g/L), and the process was carried out at  $50\text{mA}/\text{cm}^2$  for 8 min. The corrosion performance of coatings was studied using electrochemical impedance spectroscopy (EIS) which was conducted in 3.5wt% NaCl, the results are shown in Figure 13. Addition of  $\text{Na}_3\text{AlF}_6$  can improve the corrosion resistance of PEO coatings compared to that without  $\text{Na}_3\text{AlF}_6$ . However, increasing the concentration of  $\text{Na}_3\text{AlF}_6$  from 1.5 g/L to 3 g/L lead to decrease of the corrosion resistance, which is caused by higher porosity and micro pores in the PEO coatings grown at high concentration of  $\text{Na}_3\text{AlF}_6$ . Apparently, the amount of the additives needs to be optimized.

**b) Mechanical Properties of PEO coatings:** The mechanical properties of PEO coatings depends largely on phase composition, morphology and structure. For example, high hardness and excellent wear resistance can be achieved in coatings with high content of  $\alpha\text{-Al}_2\text{O}_3$  [66]. The hardness is also dependent on the level of porosity and micro-cracks present. Previous studies have shown that hardness of PEO coatings on aluminum alloy can reach 900-2000Hv [66,98]. In PEO coatings, the hardness of the alumina phases,  $\alpha\text{-Al}_2\text{O}_3$ ,  $\gamma\text{-Al}_2\text{O}_3$ , and mullite are about 26GPa, 17GPa, and 10.5GPa respectively, for amorphous phases formed through anodic oxidation the hardness is 7GPa [64,66,96]. The  $\gamma\text{-Al}_2\text{O}_3$  phase is metastable and can easily transform to  $\alpha\text{-Al}_2\text{O}_3$  at high temperatures of 800 to 1200°C. This makes it possible to control the level of  $\alpha\text{-Al}_2\text{O}_3$  to achieve higher hardness in PEO coatings.

**Table 3:** Comparison of convectional anodizing and PEO process [24,29,55,66-67].

Property	Convectional Anodizing	PEO Technology
Current density, $\text{A dm}^{-2}$	<10	<30
Cell voltage, V	20-80	100-800
Substrate pretreatment	Critical	Less critical
Electrolytes	acid	Neutral/alkaline
Oxide thickness, $\mu\text{m}$	<10	<200
Maximum scale	Can be $>1000 \text{ m}^2\text{day}^{-1}$	Usually $<10 \text{ m}^2\text{day}^{-1}$
Alloys coatings	Relatively poor	Improved
Temperature control	Critical	Not too important
Micro hardness (HV)	$\leq 500$	$\leq 1400\text{-}1700$
Adhesion to substrate	Moderate	Very high
Fatigue limit ( $10^7$ cycles)/MPa	100-210	160-270
Energy consumption/( $\text{KWhm}^{-2}\mu\text{m}^{-1}$ )	0.1-0.5	3-26.7
Corrosion resistance (relative)	Good (1)	Excellent (5)
Wear Resistance (relative)	Fair (2)	Excellent (30)

**Applications of PEO coatings:** Plasma electrolytic oxidation coatings are currently produced and distributed worldwide by some industries, this include Keronite (UK), CeraFuse (CCT1, USA), Mofratech/Ceratronix (France), Machaon (Torset, Russia), Magoxid-Coat (AHC, Germany), and Tagnite (Tag. Inc., USA) [29,74]. PEO coatings have found applications in many sectors, including aerospace, automobile, oil and gas processing, electrical,

Also, PEO coatings prepared on aluminum substrate containing Cu mostly have higher content of  $\alpha\text{-Al}_2\text{O}_3$  (~60%), while  $\gamma\text{-Al}_2\text{O}_3$  is the most dominant in the case of aluminum substrate containing Mg [66,99]. This is one of the reasons why PEO coatings prepared on different aluminum alloys exhibit significant differences in hardness. In previous studies the hardness of PEO coatings are mostly determined using Vickers hardness tester, eddy current gage, and light microscopy [60,71,84]. Interestingly, previous studies have also shown that abrasive wear rate of PEO coated 6061 alloy can be improve by a factor of 12-30, while hard anodizing can only improve by a factor 2, this makes it possible to replace steel and cast-iron parts in automotive and aircraft industry with PEO coated AA 6061 alloys [66,100]. The resistance of Al and Al alloys to fatigue loading is another challenging area that needs more attention. This problem is a surface phenomenon and is mainly caused by nucleation of crack and crack growth. There has been a huge interest employing surface treatment methods or coating technologies to reduce fatigue challenges of Al alloys, unfortunately less work has been done so far [74], and obviously more research should be conducted to study the fatigue of PEO-coated Al alloys.

PEO technique produces thick and hard ceramic coatings with strong surface compactness and adhesion to substrate. A comparison of process conditions and coating properties of PEO technique and conventional anodizing technique is summarized in Table 3.

construction, and biomedical industries, typical examples are shown in Table 4. The significant use of PEO coatings in these sectors is because of their unique properties which include high hardness, excellent corrosion and wears resistance, strong adhesion to substrate, high heat resistance, high dielectric constant, and biocompatibility [75-76] (Table 4).

**Table 4:** Examples of industrial applications of PEO coatings [29, 61, 66, 77].

Substrate	Major Component	Thickness	Industrial Sector
Al	$\gamma$ -Al <sub>2</sub> O <sub>3</sub>	50-100	Aerospace industry (valve bodies/actuators)
Al-Si	Mullite	100-150	Automotive engines (pistons/cylinder liners)
AA7075	$\alpha$ -Al <sub>2</sub> O <sub>3</sub>	15-60	Aerospace industry
Al-Mg	$\gamma$ -Al <sub>2</sub> O <sub>3</sub>	60-120	Gas and oil extraction (seals/rings)
Al	$\gamma$ -Al <sub>2</sub> O <sub>3</sub>	30-80	Tools manufacture (cutting/sharpening)
High strength Al	$\alpha$ -Al <sub>2</sub> O <sub>3</sub>	100-150	Textile processing (rotors/rollers)

## Conclusion and Prospects

Anodic oxidation and plasma electrolytic oxidation have been widely employed for surface enhancement on aluminum and aluminum alloys. Compared to conventional anodization process, PEO process offers excellent improvement in mechanical properties due to the unique microstructure of the PEO coatings. PEO coatings have high hardness, excellent adhesion to substrate and exhibit high thermal resistivity. Because of the porous external layer of the PEO coatings, the corrosion resistance of the PEO coatings needs to be improved. Sealing using organic and inorganic dyes to block pores and cracks is widely adopted in conventional anodizing technique, which can be explored for PEO coatings. The PEO technique is environmentally friendly compared to hard-anodizing technique. The phase composition, structure, morphology as well as corrosion performance and mechanical properties of PEO coatings can be influenced largely by process parameters such as substrate material, electrolyte composition and temperature, addition of additives, growth time, and electrical parameters such as current density, current frequency, duty cycle, and anodic and cathodic voltage. All these variables give us the opportunity to tune the PEO process, but meanwhile needs great effort to optimize the process. The recent development on artificial intelligent and machine learning may help to shorten the optimization process. The merits of PEO coatings make it very attractive for many applications ranging from aerospace to automobile and to consumer electronics. In order to make the PEO technology more industry ready and appealing, more in-depth research on understanding the growth mechanism by both in-situ and ex-situ techniques, controlling the microstructure and properties of the PEO coatings, optimizing process parameters, developing sealing technology, and developing more innovative PEO process are needed.

## Acknowledgement

XH acknowledges the support from A\*STAR Aerospace Program, Singapore.

## Conflict of Interest

They authors declares that they have no conflict of interests.

## References

- J Staley, D Lege (1993) Advances in aluminum alloy products for structural application in transportation. *Journal de Physique IV Colloque 03(C7)*: 179-190.
- M Arif, M Asif, I Ashmed (2017) Advanced composite material for aerospace application-a review. *Int J Eng Mfg Sci 7(2)*: 393-409.
- EA Starke, Jr JT Staley (1996) Application of modern aluminum alloys to aircrafts. *Prog Aerosp Sci 32(2-3)*: 131-172.
- RC Dorward, TR Pritchett (1988) Advanced aluminum alloys for aircraft and aerospace applications. *Materials & Design 9(2)*: 63-69.
- KA Yasakau, ML Zheludkevich, MGS Ferreira (2018) *Intermetallic Matrix Composites*, Woodhead Publishing, UK, pp. 425.
- TSM Mui, LLG Silva, V Prysiashnyi, KG Kostov (2017) Surface modification of aluminum alloys by atmospheric pressure plasma treatments for enhancement of their adhesion properties. *Surf Coat Tech 312*: 32-36.
- AS Warren (2004) Development and challenges for aluminum-A Boeing perspective. *Materials Forum 28*: 24-31.
- P Rambabu, NE Prasad, VV Kutumbarao, RJH Wanhill (2017) Aluminum alloys for aerospace applications (chapter 2), *Aerospace materials and materials technologies 1*: 29-52.
- NE Prasad, AG Amol, RJH Wanhill (Eds) (2014) *Aluminum-Lithium alloys: processing, properties and applications*. Elsevier Inc, Oxford, UK.
- NL Sukiman, X Zhou, N Birbilis, AE Hughes, JMC Mol, et al. (2013) Durability and corrosion of aluminum and its alloys: Overview, property space, techniques and developments (chapter 2). pp. 48-97.
- E Salamci (2002) Mechanical properties of spray cast 7xxx series aluminum alloys. *Turkish J Eng Env Sci 26(4)*: 345-352.
- Yu-guo Liao, Xiao-qi Han, Miao-xia Zeng, Man Jin (2015) Influence of Cu on microstructure and tensile properties of 7xxx series aluminum alloys. *Mater Design 66(Part B)*: 581-586.
- L Shao, H Li, B Jiang, C Liu, X Gu, et al. (2018) A comparative study of corrosion behavior of hard anodized and micro-arc oxidation coatings on 7050 aluminum alloy. *Metals 8(3)*: 165.
- RJH Wanhill, RT Byrnes, CL Smith (2011) Stress corrosion cracking (SCC) in aerospace vehicles. In: VS Raja, T Shoji (eds) *Stress corrosion cracking. Theory and practice*. Woodhead publishing Ltd, Cambridge, UK, pp. 608-650.
- RL Twite, GP Bierwagen (1998) Review of alternatives to chromate for corrosion protection of aluminum aerospace alloys. *Prog Org Coat 33(2)*: 91-100.
- T Arunnellaiappan, LR Krishna, S Anoop, RR Uma, N Rameshbabu (2016) Fabrication of multifunctional black PEO coatings on AA7075 for space applications. *Surf Coat Tech 307*: 735-746.
- PV Kumar, B Shantanu (2017) Plasma processing of aluminum alloys to promote adhesion: A critical review. *Reviews of Adhesion and Adhesives 5(1)*: 79-104.
- HF Nabavi, M Aliofkhaezrai, AS Rouhaghdam (2017) Electrical characteristics and discharge properties of hybrid plasma electrolytic oxidation on titanium. *J Alloys Compd 728*: 464-475.
- S Ji, Y Weng, Z Wu, Z Ma, X Tian, et al. (2017) Excellent corrosion resistance of P and Fe modified micro-arc oxidation coating on Al alloy. *J Alloys Compd 710*: 452-459.
- JL Patel, N Saka (2011) Microplasmic coatings. *Am Ceram Soc Bull 80(4)*: 27-29.
- D Petković, F Živić, G Radenković, Trajanović, M Manić (2013) Coating: A way to improve biomedical properties of AISI316L stainless steel. *ICP-35*: 1-8.

22. AA Alwahib (2010) Laser surface treatment for anodizing process of aluminum alloy. *Eng Tech Journal* 28 (16): 5151-5154.
23. JMC Moreno, P Osiceanu, C Vasilescu, M Anastasescu, SL Drob, et al. (2013) Obtaining, structural and corrosion characterization of anodized nanolayers on Ti-20Zr alloy surface. *Surf Coat Technol* 235: 782-802.
24. FC Walsh, CTJ Low, RJK Wood, KT Stevens, J Archer, et al. (2009) Plasma electrolytic oxidation (PEO) for production of anodized coatings on lightweight metals (Al, Mg, Ti) alloys. *TI Met Finish* 87(3): 122-134.
25. ZM Yan, TW Guo, HB Pan, JJ Yu (2002) Influence of electrolyzing voltage on chromatics of anodizes titanium dentures. *Mater Trans* 43(12): 3142-3145.
26. G Napoli, M Paura, T Vela, A Di Schino (2018) Coloring titanium alloys by anodic oxidation. *Metabk* 57(1): 111-113.
27. P Michal, A Vagaská, E Fehová, M Gombár, D Kozak (2016) Effect of electrolyte temperature on the thickness of anodic aluminum oxide (AAO) layer. *Metabk* 55(3): 403-406.
28. W Gumowska, I Bobosz, B Wrzozszyk (2014) The morphology of the alumina films formed in the anodization process of alumina in the phosphoric acid solution. *Arch Metall Mater* 59(1): 137-143.
29. Q Li, J Liang, Q Wang (2013) Plasma electrolytic oxidation coatings on lightweight metals (chapter 4). *Modern Surface Engineering Treatments* pp. 75-99.
30. ZB Yang, JC Hu, KQ Li, SY Zhang, QH Fan, et al. (2017) Advances of the research evolution on aluminum electrochemical anodic oxidation technology. *IOP Conf Series: Mater Sci Eng* 283(conference 1): 012003.
31. D Elabar, GR La Monica, M Santamaria, F Di Quarto, P Skeldon, et al. (2017) Anodizing of aluminum and AA 2024-T3 alloy in chromic acid: Effect of sulphate on film growth. *Surf Coat Technol* 309: 480-489.
32. VM Dumitrascu, L Benea, NL Simionescu (2018) Evaluation of sealing process on the surface properties of nanoporous aluminum oxide layers electrochemically growth on 1050 aluminum alloys surface. *IOP Conf Series: Mater Sci Eng* 374 (conference 1): 012013.
33. Y Wan, H Wang, Y Zhang, X Wang, Y Li (2018) Study on Anodic Oxidation and Sealing of Aluminum Alloy. *Int J Electrochem Sci* 13: 2175-2185.
34. KS Napolskii, IV Roslyakov, AA Eliseev, DV Byelov, AV Petukhov, et al. (2011) The kinetics and mechanism of long-range pore ordering in anodic films on aluminum. *J Phys Chem C* 115(48): 23726-23731.
35. W Lee (2010) The anodization of aluminum for nanotechnology applications. *JOM* 62(6): 57-63.
36. C Cheng, AHW Ngan (2015) Theoretical pore growth models for nanoporous alumina. *Nanoporous Alumina*, chapter 2, pp. 31-60.
37. Y Shang, L Wang, D Niu, Z Liu, Y Wang, et al. (2016) Effect of additive for anodizing electrolyte on anodic film of high silicon aluminum alloy. *Int J Electrochem Sci* 11(2016): 1549-1557.
38. MV Diamanti, MP Pedferri (2007) Effect of anodic oxidation parameters on titanium oxides formation. *Corros Sci* 49(2): 939-948.
39. MV Diamanti, BD Curto, M Pedferri (2011) Anodic oxidation of titanium: from technical aspects to biomedical applications. *J App Biomater Biomech* 9(1): 55-69.
40. TI Devyatkina, EI Yarovaya, VV Rogozhin, TV Markova, MG Mikhaleenko (2014) Anodic oxidation of complex shaped items of aluminum and aluminum alloys with subsequent electrodeposition of copper coatings. *Russian J Appl Chem* 87(1): 54-60.
41. M Ardelean, S Lascau, E Ardelean, A Josan (2018) Surface treatments of aluminum alloys. *IOP Conf Series: Mater Sci Engineer* 294(conference 1): 012042.
42. N Hu, X Dong, X He, JF Browning, DW Schaefer (2015) Effect of sealing on the morphology of anodized aluminum oxide. *Corros Sci* 97: 17-24.
43. TS Shih, TH Lee, YJ Jhou (2014) The effect of anodization on the microstructure and fatigue behavior of 7075-T3 aluminum alloy. *Mater Trans* 55(8): 1280-1285.
44. L Hao, BR Cheng (2000) Sealing processes of anodic coatings-past, present, and future. *Metals Finishing* 98(12): 8-18.
45. AMA El-Hameed, YA Abdel-Aziz, FS El-Tokhy (2017) Anodic coating characteristics of different aluminum alloys for spacecraft materials applications. *Matl Sci Appl* 8: 197-208.
46. M Moradi, M Noormohammadi, F Behzadi (2011) Three-dimensional structural engineering of nanoporous alumina by controlled sprinkling of an electrolyte on a porous anodic alumina (PAA) template. *J Phys D: Appl Phys* 44(4): 1-7.
47. RDZ Montoya, EL Vera, YT Pineda, ML Cedeno (2017) Effect of the layer of anodized 7050-T6 aluminum corrosion properties. *J Phys: Conf Ser* 786(1): 012032.
48. R Elaish, M Curioni, K Gowers, A Kasuga, H Habazaki, et al. (2017) Influence of fluorozirconic acid on sulfuric acid anodizing of aluminum. *J Electrochem Soc* 164(13): 831-839.
49. ST Abrahami, JMM de Kok, VC Gudla, R Ambat, H Terryn, et al. (2017) Interface strength and degradation of adhesively bonded porous aluminum oxides. *NPJ Materials Degradation*, pp. 1-8.
50. WJ Stepniowski, Z Bojar (2011) Synthesis of anodic aluminum oxide (AAO) at relatively high temperatures. Study of the influence of anodization conditions on the alumina structural features. *Surf Coat Technol* 206(2-3): 265-272.
51. Y Cheng, F Wu, J Dong, X Wu, Z Xue, et al. (2012) Comparison of plasma electrolytic oxidation of Zirconium alloy in silicate- and aluminate-based electrolytes and wear properties of the resulting coatings. *Electrochim Acta* 85: 25-32.
52. A Sharma, YJ Jang, JP Jung (2017) Effect of KOH to Na<sub>2</sub>SiO<sub>3</sub> ratio on microstructure and hardness of plasma electrolytic oxidation coatings on AA 6061 alloy. *J Mater Eng Perform* 26(10): 5032-5042.
53. T Arunnellaiappan, NK Badu, LR Krishna, N Rameshbabu (2015) Influence of frequency and duty cycle on microstructure of plasma electrolytic oxidized AA7078 and correlation to its corrosion behavior. *Surf Coat Technol* 280: 136-147.
54. DS Tsai, CC Chou (2018) Review of the soft sparking issues in plasma electrolytic oxidation. *Metals* 8(2): 1-22.
55. E Matykina, R Arrabal, M Mohedano, B Mingo, J Gonzalez, et al. (2017) Recent advances in energy efficient PEO processing of aluminum alloys. *Trans Nonferrous Met Soc China* 27(7): 1439-1454.
56. RO Hussein, X Nie, DO Northwood, A Yerokhin, A Mathews (2010) Spectroscopic study of electrolytic plasma and discharging behavior during the plasma electrolytic oxidation (PEO) process. *J Phys D Appl Phys* 43(10): 105203-105216.
57. W Gebarowski, S Pietrzyk (2013) Influence of the cathodic pulse on the formation and morphology of oxide coatings on aluminum produced by plasma electrolytic oxidation. *Arch Metall Mater* 58(1): 241-245.
58. E Erfanifar, M Aliofkhaezrai, HF Nabavi, AS Roughghadam (2017) Growth kinetics and morphology of micro-arc oxidation coating on aluminum. *Surf Coat Technol* 185: 162-175.
59. G Sundararajan, L Rama (2003) Mechanisms underlying the formation of thick alumina coatings through the MAO coating technology. *Surf Coat Technol* 167(2-3): 269-277.
60. EA Akbar, MA Qaiser, A Hussain, RA Mustafa, D Xiong (2017) Surface modification of aluminum alloy 6060 through plasma electrolytic oxidation. *Int J Eng Works* 4(6): 114-123.
61. V Dehnav. (2014) Surface modification of aluminum alloys by plasma electrolytic oxidation. PhD Thesis, The University of Western Ontario, Canada.
62. LO Snizhko, AL Yerokhin, A Pilkington, NL Gurevina, DO Misnyankin, et al. (2004) Anodic processes in plasma electrolytic oxidation of aluminum in alkaline solutions. *Electrochim Acta* 49(13): 2085-2095.
63. L Agureev, S Savushkina, A Ashmarin, A Borisov, A Apfeld, et al. (2018) Study of plasma electrolytic oxidation coatings on aluminum composites. *Metals* 8(459): 1-12.



64. V Dehnavi, XY Liu, BL Luan, DW Shoesmith, S Rohani (2014) Phase transformation in plasma electrolytic oxidation coatings on 6061 aluminum alloys. *Surf Coat Technol* 251: 106-114.
65. LO Snizhko, AL Yerokhin, NL Gurevina, V Patalakha, A Matthews (2007) Excessive oxygen evolution during plasma electrolytic oxidation of aluminum. *Thin Solid Films* 516(2-4): 460-464.
66. RO Hussein, DO Northwood (2014) Production of anti-corrosion coatings on light alloys (Al, Mg, Ti) by plasma-electrolytic oxidation (PEO) (chapter 11), pp. 202-238.
67. AL Yerokhin, A Shatrov, V Samsonov, P Shashkov, A Pilkington, et al. (2005) Oxide ceramic coatings on aluminum alloy produced by a pulse bipolar plasma electrolytic oxidation process. *Surf Coat Technol* 199(2): 150-157.
68. X Liu, S Wang, N Du, Q Zhao (2018) Evolution of the three-dimensional structure and growth model of plasma electrolytic oxidation coatings on 1060 aluminum alloy. *Coatings* 8(3): 1-13.
69. GP Wirtz, SD Brown, WM Kriven (1981) Materials manufacture processes, 6(87).
70. MK Sharma, Y Jang, J Kim, H Kim, JP Jung (2014) Plasma electrolytic oxidation in surface modification of metals for electronics. *J Welding and Joining* 32(3): 27-33.
71. QP Tran, TS Chin (2016) Plasma electrolytic oxidation coating on 6061Al alloy using an electrolyte without alkali ions. *J Sci Technol* 54(5A): 151-158.
72. JA Curran, H Kalkanci, Yu Magurova, TW Clyne (2007) Mullite-rich plasma electrolytic oxide coatings for thermal barrier applications. *Surf Coat Technol* 201(21): 8683-8687.
73. NY Dudareva, MM Abramova (2016) The structure of plasma-electrolytic coating formed on Al-Si alloys by the micro-arc oxidation method. *Prot Met* 52(1): 128-132.
74. TW Clyne, SC Troughton (2018) A review work on discharge characteristics during plasma electrolytic oxidation of various metals. *International materials reviews* 64(3): 127-162.
75. LR Krishna, KRC Somaraju, G Sundararajan (2003) The tribological performance of ultra-hard ceramic composite coatings obtained through micro-arc oxidation. *Surf Coat Technol* 163-164: 484-490.
76. M Mohedano, E Matykina, R Arrabal, B, Mingo, A Pardo (2015) PEO of pre-anodized Al-Si alloys: corrosion properties and influence of sealings. *Appl Surf Sci* 346: 57-67.
77. S Shrestha, BD Dunn (2007) Advanced plasma electrolytic oxidation treatment for protection of light weight materials and structures in a space environment. *Surface World*, pp. 40-44.
78. MMS Al Bosta, KJ Ma, HH Chien (2013) Effect of anodic current density on characteristics and low temperature IR emissivity of ceramic coating on aluminum 6061 alloy prepared by micro-arc oxidation. *J Ceram* 2013: 1-14.
79. Y Gencer, M Tarakci, AE Gulec, ZC Oter (2014) Plasma electrolytic oxidation of binary Al-Sn alloy. *Acta Physica Polonica A* 125(2): 659-663.
80. L Sottovia, MLP Antunes, CA Antonio, EC Rangel, N Christino da Cruz (2014) Thin films produced on 5052 aluminum alloy for plasma electrolytic oxidation with red mud-containing electrolytes. *Materials Research* 17(6): 1404-1409.
81. Y Zhang, W Fan, HQ Du, YW Zhao (2017) Corrosion behavior and structure of plasma electrolytic oxidation coated aluminum alloy. *Int J Electrochem Sci* 12(2017): 6788-6800.
82. JZ Li, ZC Shao, YW Tian, FD Kang, YC Zhai (2004) Application of micro-arc oxidation for Al, Mg, Ti and their alloys. *Corrosion Science and Protection Technology* 16(4): 218-221.
83. JM Oh, JI Mum, JH Kim (2009) Effects of alloying elements on microstructure and protective properties of Al<sub>2</sub>O<sub>3</sub> coatings formed on aluminum alloy substrates by plasma electrolysis. *Surf Coat Technol* 204(1-2): 141-148.
84. M Sieber, F Simchen, R Morgenstern, I Scharf, T Lampke (2018) Plasma electrolytic oxidation of high-strength aluminum alloys-substrate effect on wear and corrosion performance. *Metals* 5(356): 1-17.
85. KR Shin, YG Ko, DH Shin (2011) Effect of electrolyte on surface properties of pure titanium coated plasma electrolytic oxidation. *J Alloys Compd* 509(Supplement 1): 478-481.
86. Gh Barati Darband, M Aliofkhaezrai, P Hamghalam, N Valizade (2017) Plasma electrolytic oxidation of magnesium and its alloys: Mechanism, properties and applications. *Journal of Magnesium and Alloys* 5(1): 1-58.
87. H Sharif, M Aliofkhaezrai, GB Darband (2018) A review on adhesion strength of PEO coatings by scratch test method. *Surf Rev Lett* 25(7): 1830004.
88. XD Chen, QZ Cai, LS Yin (2012) Effect of Na<sub>2</sub>WO<sub>4</sub> additive on properties of plasma electrolytic oxidation coatings on 6061 Al alloy. *Advances Materials Research* 550-553: 1969-1975.
89. IJ Hwang, KR Shin, JS Lee, YG Ko, DH Shin (2012) Formation of black ceramic layer on aluminum alloy by plasma electrolytic oxidation in electrolyte containing Na<sub>2</sub>WO<sub>4</sub>. *Materials Transactions*, 53(3): 559-564.
90. X Wang, X Wu, R Wang, Z Qui (2013) Effect of Na<sub>3</sub>AlF<sub>6</sub> on the structure and mechanical properties of plasma electrolytic oxidation coatings on 6061 Al alloy. *Int J Electrochem Sci* 8: 4986-4995.
91. M Kaseem, HW Yang, YG Ko (2017) Toward a nearly defect-free coating via high-energy plasma sparks. *Sci Rep* 7(1): 2378.
92. A Ayday, M Durman (2015) Growth characteristics of plasma electrolytic oxidation coatings on aluminum alloys. *Acta Physica Polonica* 127(4): 886-887.
93. RHU Khan, AL Yerokhin, T Pilkington, A Leyland, A Mathews (2005) Residual stresses in plasma electrolytic oxidation coatings on Al alloy produced by pulsed unipolar current. *Surf Coat Technol* 200(5-6): 1580-1586.
94. BL Jiang, YM Wang (2010) Plasma electrolytic oxidation treatment of aluminum and titanium alloys in: H Dong (Ed), *Surf Eng Light Alloy, Aluminum, Magnes. Titan Alloy*, Woodhead publishing, pp. 110-153.
95. RO Hussein, P Zhang, X Nie, Y Xia, DO Northwood (2011) The effect of current mode and discharge type on the corrosion resistance of plasma electrolytic oxidation (PEO) coated magnesium alloy. *Surf Coat Technol* 206(7): 1990-1997.
96. W Xu, Q Jin, Q Zhua, M Hu, Y Ma (2009) Anti-corrosion micro-arc oxidation coatings on SiCP/AZ31 magnesium matrix composite. *J Alloys Compd* 482(1-2): 208-212.
97. JA Curran, TW Clyne (2005) Thermal-physical properties of plasma electrolytic oxide coatings on aluminum. *Surf Coat Technol* 199: 168-176.
98. E Matykina, R Arrabal, P Skeldon, GE Thompson (2009) Investigation of the growth processes of coatings by AC plasma electrolytic oxidation of aluminum. *Electrochim Acta* 54(27): 6767-6778.
99. AL Yerokhin, X Nie, A Leyland, A Matthews, SJ Dowe (1999) Plasma electrolysis for surface engineering. *Surf Coat Technol* 122(2-3): 73-93.
100. LR Krishna, AS Purnima, G Sundararajan (2006) A comparative study of tribological behavior of micro-arc oxidation and hard-anodized coatings. *Wear* 261(10): 1095-1101.
101. XH Huang, L Li, X Luo, XG Zhu, GH Li (2018) Orientation-controlled synthesis and ferromagnetism of single crystalline Co nanowire arrays. *J Phys Chem C* 112(5): 1468-1472.